Journal of Alloys and Compounds 509 (2011) 6696–6699

Contents lists available at ScienceDirect

Journal of Alloys and Compounds

journal homepage: www.elsevier.com/locate/jallcom

Growth, crystal structure and optical properties of layered dibarium cadmium diborate, $Ba_2Cd(BO_3)_2$

Min Zhang[a,b], Shilie Pan[a,*], Jian Han[a], Yun Yang[a,b], Liang Cui[a,b], Zhongxiang Zhou[a]

[a] Xinjiang Key Laboratory of Electronic Information Materials and Devices, Xinjiang Technical Institute of Physics & Chemistry, Chinese Academy of Sciences, Urumqi 830011, China
[b] Graduate University of Chinese Academy of Sciences, Beijing 100049, China

ARTICLE INFO

Article history:
Received 30 December 2010
Received in revised form 18 March 2011
Accepted 24 March 2011
Available online 31 March 2011

Keywords:
$Ba_2Cd(BO_3)_2$
Crystal structure
Crystal growth
Borate

ABSTRACT

A novel dibarium cadmium diborate, $Ba_2Cd(BO_3)_2$, has been successfully synthesized by standard solid-state reaction. Large sheet-like crystal with size up to 20 mm × 15 mm × 0.7 mm has been obtained using top-seed solution growth method. $Ba_2Cd(BO_3)_2$ crystallizes in the monoclinic space group $C2/m$ with $a = 9.6305(4)$ Å, $b = 5.3626(3)$ Å, $c = 6.5236(2)$ Å, $\beta = 118.079(3)^\circ$, $Z = 2$. The crystal structure is composed of isolated $[BO_3]$ triangles, $[CdO_6]$ octahedra and $[BaO_9]$ polyhedra. CdO_6 are vertex-connected with six BO_3 to form infinite $_\infty[Cd(BO_3)_2]$ layers extending in (0 0 1) plane, and two rows of Ba atoms closely occupy two side of $_\infty[Cd(BO_3)_2]$ layers to forming stoichiometric sheets. IR and transmittance spectrum of $Ba_2Cd(BO_3)_2$ were reported.

1. Introduction

Crystal chemistry of borates differs from those of silicates, phosphates, sulfates, carbonates and nitrates, because anionic radicals in the borate can be both B-tetrahedra and B-triangles [1–4]. Especially, the metal borates with potentially useful physical properties ranging from nonlinear optical (NLO), ferroelectric, piezoelectric to semiconducting behaviors, are of continuing interest [5–8]. Since the discovery of the excellent NLO crystals such as β-BaB_2O_4 [9], $KBe_2BO_3F_2$ (KBBF) [10] and $Sr_2Be_2B_2O_7$ (SBBO) [11], alkaline-earth metal borates have been extensively studied. In searching for non-centrosymmetric (NCS) oxides, much attention has been paid to combine boron–oxygen units with other NCS as a binary building unit in the syntheses of NLO materials. Mostly researched NCS chromophores are oxides containing second-order Jahn–Teller (SOJT) distorted cations such as d^0 transition metal ions (Ti^{4+}, Nb^{5+}, W^{6+}, etc.) and cations with a lone pair electrons of ns^2 (Sn^{2+}, Se^{4+}, Te^{4+}, Bi^{3+}, etc.) [12–17]. In recent decades, some significant investigations have been studied on d^{10} cations (Cd^{2+}, Zn^{2+}, etc.), whose polar displacement is likely to lead an asymmetric bonding configuration [18–20].

However, to our best knowledge, there is no report on the mixed borates in M_2O–CdO–B_2O_3 (M = alkaline-earth metal) systems until now. We have, therefore, started investigating these systems. Extensive efforts in the ternary M_2O–CdO–B_2O_3 systems led to a new phase, $Ba_2Cd(BO_3)_2$. Herein we report its synthesis, growth, crystal structure, and optical properties for the first time.

2. Experimental

2.1. Crystal growth and compound synthesis

Single crystals of $Ba_2Cd(BO_3)_2$ were grown by the top-seeded solution growth (TSSG) method in a PbO–PbF_2 with excess H_3BO_3 and CdO flux system. All reagents were of analytical grade, H_3BO_3 (7.4196 g, 0.12 mol), CdO (7.7046 g, 0.06 mol), $Ba(NO_3)_2$ (15.6804 g, 0.06 mol), PbO (6.6960 g, 0.03 mol) and PbF_2 (7.3560 g, 0.03 mol) were precalcined at 300 °C for 4 h and 600 °C for 8 h, respectively, to decompose the boric acid and barium nitrate. The mixture was heated to 850 °C and kept for 10 h to ensure that the powder was melted into solution completely and mixed homogeneously, then cooled down to 760 °C at a rate of 10 °C/h. And seed crystal was introduced into liquid surface for 20 min to dissolve the outer surface. Then it was quickly cooled down to 740 °C and followed by a slow cooling at a rate of 0.5 °C/day until the desired size was obtained.

The title compound was synthesized by solid-state reaction method. Stoichiometric mixture of H_3BO_3 (1.2366 g, 0.02 mol), CdO (1.2841 g, 0.01 mol) and $Ba(NO_3)_2$ (5.2668 g, 0.02 mol) were mixed homogeneously gradually heated to 800 °C, and kept at this temperature for 60 h with several intermediate grindings and mixings. X-ray powder diffraction data were collected using Bruker D2 PHASER diffractometer.

2.2. Structure determination

Single-crystal X-ray intensity data were collected on a Bruker SMART APEX II single-crystal diffractometer at 296(2) K using Mo Kα radiation (λ = 0.71073 Å) and integrated with a SAINT-Plus program [21]. The crystal structure was solved by direct methods and refined in SHELX-97 system [22]. Final least-squares refinement on F_o^2 with data having $F_o^2 \geq 2\sigma(F_o^2)$ includes anisotropic displacement parameters for all atoms. Unit cell parameters were derived from a least-squares analysis of 1391 reflections in the range 3.54–27.56°. The final difference Fourier synthesis map

* Corresponding author. Tel.: +86 991 3674558; fax: +86 991 3838957.
E-mail address: slpan@ms.xjb.ac.cn (S. Pan).

0925-8388/$ – see front matter © 2011 Elsevier B.V. All rights reserved.
doi:10.1016/j.jallcom.2011.03.141

Table 1
Crystal data and structure refinement for $Ba_2Cd(BO_3)_2$.

Empirical formula	$Ba_2Cd(BO_3)_2$
Formula weight	504.70
Temperature (K)	296(2)
Crystal system	Monoclinic
Space group	$C2/m$ (No. 12)
Unit cell dimensions	
a (Å)	9.6305(4)
b (Å)	5.3626(3)
c (Å)	6.5236(2)
β (°)	118.079(3)
Volume (Å^3)	297.25(2)
Z	2
Density (calcd) (g/cm^3)	5.639
Absorption coefficient (mm^{-1})	16.611
F(000)	436
Crystal size (mm^3)	0.069 × 0.125 × 0.216
θ Range for data collection (°)	3.54–27.56
limiting indices	$-12 \le h \le 12$, $-6 \le k \le 6$, $-8 \le l \le 8$
Reflections collected/unique	1391/379 [R(int) = 0.0320]
Completeness to θ = 27.56° (%)	99.2
Refinement method	Full-matrix least-squares on F^2
Data/restraints/parameters	379/0/33
GOF on F^2	1.251
Final R indices [$I > 2\sigma(I)$][a]	$R1$ = 0.0269, $wR2$ = 0.0775
R indices (all data)[a]	$R1$ = 0.0274, $wR2$ = 0.0778
Extinction coefficient	0.0081(11)
Largest diff peak and hole (e/Å^3)	1.666 and −1.587

[a] $R_1 = \Sigma||F_o| - |F_c||/\Sigma|F_o|$ and $wR_2 = [\Sigma w(F_o^2 - F_c^2)^2/\Sigma w F_o^4]^{1/2}$ for $F_o^2 > 2\sigma(F_o^2)$.

showed the maximum and minimum peaks at 1.666 and −1.587 e/Å^{-3}, respectively. The structure was checked for missing symmetry elements with PLATON [23].

2.3. IR spectrum

The infrared spectrum was carried out on a Shimadzu IRAffinity-1 spectrometer in order to specify and compare the coordination of boron in $Ba_2Cd(BO_3)_2$. The synthesized sample was mixed thoroughly with dried KBr (5 mg of the sample and 500 mg of KBr), and the spectrum was collected in the range from 400 to 4000 cm^{-1} with a resolution of 2 cm^{-1}.

2.4. Transmission spectrum

The transmission spectrum of the $Ba_2Cd(BO_3)_2$ crystal was measured using crystal sample plate at room temperature on a Shimadzu SolidSpec-3700DUV UV–VIS–IR Spectrophotometer. The crystal plate was obtained by cutting the as-grown crystal and without polishing, and its thickness was about 0.7 mm. The measurement range extended from 190 to 2600 nm.

3. Results and discussion

3.1. Description of crystal structure

Single-crystal X ray diffraction date show that $Ba_2Cd(BO_3)_2$ crystallizes in the monoclinic system with space group $C2/m$. Crystal data and structure refinement are listed in Table 1; atomic coordinates and equivalent isotropic displacement parameters are listed in Table 2; selected bond lengths and angles are list in Table 3. The basic structure units in $Ba_2Cd(BO_3)_2$ are isolated CdO_6 octahedra and BO_3 triangles (Fig. 1). Each CdO_6 octahedron is vertex-connected to six [BO_3] anionic groups, while every [BO_3] is shared by three CdO_6 octahedra, forming infinite $_\infty$[$Cd(BO_3)_2$] layers along (0 0 1) plane. In addition, $_\infty$[$Cd(BO_3)_2$] layers were interconnected with two rows of Ba atoms through coordination with oxygen atoms to form stoichiometric layers, resulting in the formula $Ba_2Cd(BO_3)_2$ (Fig. 2). The XRD pattern of as-grown crystal and synthesized compound with stoichiometric mixture are shown in Fig. 3 and Fig. S2, respectively. The above two XRD patterns are in good agreement with the corresponding calculated one, which further confirms the refined crystal structure. Note that the intensity difference for some diffraction lines between the two patterns

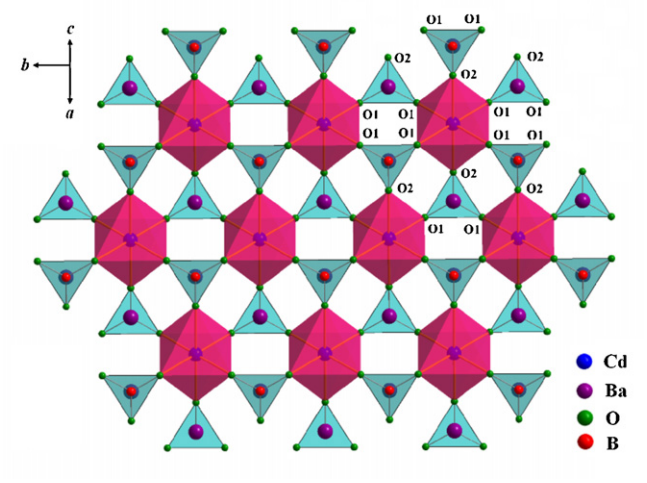

Fig. 1. A single $_\infty$[$Cd(BO_3)_2$]$^{4-}$ layer in the $Ba_2Cd(BO_3)_2$. BO_3 triangles and CdO_6 octahedra are shaded in blue and red, respectively. (For interpretation of the references to color in this figure legend, the reader is referred to the web version of this article.)

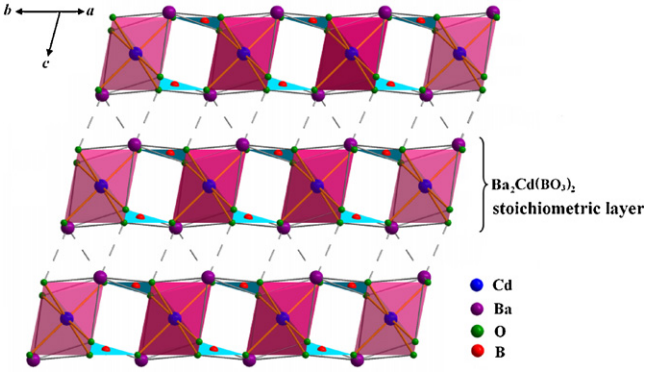

Fig. 2. The stoichiometric layer structure of $Ba_2Cd(BO_3)_2$. BO_3 triangles and CdO_6 octahedra are shaded in blue and red, respectively. (For interpretation of the references to color in this figure legend, the reader is referred to the web version of this article.)

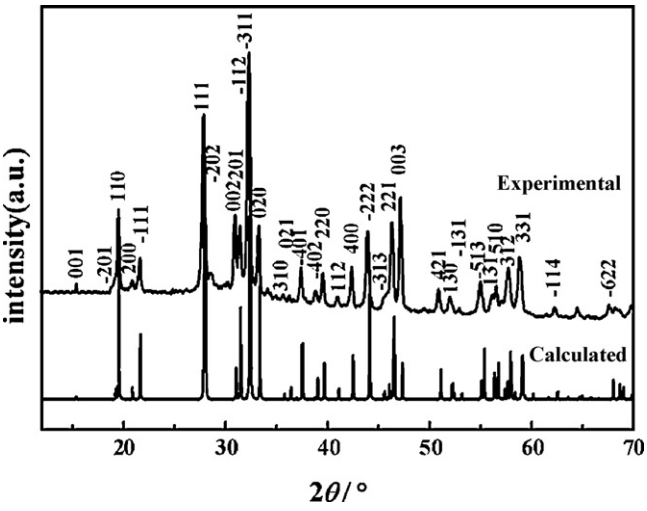

Fig. 3. Experimental and calculated XRD patterns of $Ba_2Cd(BO_3)_2$ (note: the experimental XRD pattern was collected using as-grown crystal sample).

Table 2
Atomic coordinates, equivalent isotropic displacement parameters and bond valence sum for $Ba_2Cd(BO_3)_2$. *U*(eq) is defined as one third of the trace of the orthogonalized *Uij* tensor.

Atoms	Wyckoff positions	*x*	*y*	*z*	*U*(eq)	BVS
Cd(1)	2*a*	0.0000	1.0000	1.0000	0.015(1)	2.038
Ba(1)	4*i*	0.2100(1)	1.0000	0.6879(1)	0.016(1)	2.161
B(1)	4*i*	0.0619(14)	0.5000	0.7590(20)	0.014(2)	2.907
O(1)	8*j*	−0.0214(7)	0.7224(11)	0.7255(10)	0.020(1)	2.061
O(2)	4*i*	0.2180(10)	0.5000	0.8255(17)	0.027(2)	1.965

is caused by preferred orientation of the powder sample during collection of the experimental XRD data.

In this structure, isolated planar BO_3 are distributed parallelly along two different directions. Considering the anisotropy polarizability of planar BO_3 groups, it is likely to be a promising birefringent crystal. The BO_3 triangle is slightly distorted as shown by the B–O distances and O–B–O angles (Table 3) but remains nearly planar (sum of O–B–O angles equal 360.01°). Bond valence sum (BVS) calculation using Brown's formula [24] for B^{3+} cation is also reasonable, lying in 2.907 (Table 2).

The Cd atoms are surrounded by four O atoms at distance of 2.262(6) Å, and two O atoms at distance of 2.400(9) Å, forming CdO_6 octahedra, while CdO_6 octahedra are slightly distorted indicated by the bond angles (Table S1 in Supporting Information). The average distances of Cd–O is 2.309 Å, which are very reasonable when compared with the range 2.278(14)–2.338(14) Å (average 2.312 Å, coordination number (CN) = 6) of Cd(1) and 2.263(14)–2.831(4) Å (average 2.459 Å, CN = 7) of Cd(2) in $Cd_4BiO(BO_3)_3$ [16], or 2.284(4)–2.389(4) Å (average 2.345, CN = 6) in $[Ni(H_2O)_4]Cd(VO)(PO_4)_2$ [25]. The calculated BVS value of 2.038 for Cd^{2+} is very reasonable.

The Ba atoms have a typical coordination environment with nine O atoms to form BaO_9 polyhedra, therein seven O atoms are provided by one $_\infty[Cd(BO_3)_2]$ layer and two weak bonding O atoms are from neighboring layers. Since the layered nature of the structure and weak bonding interactions between two adjacent layers, the crystal has a layered growth habit observed in the experiment (the crystal picture is shown in Fig. 4). The distances of Ba–O vary within the range of 2.753(5)–2.913(10) Å (average 2.809 Å), which agree well with the range of 2.629(3)–3.026(4) Å (average 2.802 Å, CN = 8) in $LiBa_2B_5O_{10}$ [26], 2.710(6)–3.042(11) Å (average 2.843 Å, CN = 9) in $BaBiBO_4$ [27]. Bond valence analysis of 2.161 for Ba^{2+} verifies that the Ba atoms are slightly overbonding.

As illustrated in Fig. 5, the Ba atoms are occupied in the tunnels that are enveloped by vertex-connected CdO_6 octahedra and BO_3. This kind of surroundings offers a possibility to stabilize a bivalent rare-earth ion without reducing atmosphere, for example, Eu^{2+} [28–30], then photoluminescence can be found in the doped compounds.

Table 3
Selected bond lengths (Å) and angles (°) for $Ba_2Cd(BO_3)_2$.[a]

Ba(1)–O(1)$^{\#1}$	2.753(6)	Cd(1)–O(1)	2.262(6)
Ba(1)–O(1)$^{\#2}$	2.753(5)	Cd(1)–O(1)$^{\#3}$	2.262(6)
Ba(1)–O(1)	2.785(6)	Cd(1)–O(1)$^{\#8}$	2.262(6)
Ba(1)–O(1)$^{\#3}$	2.785(6)	Cd(1)–O(1)$^{\#9}$	2.262(6)
Ba(1)–O(2)	2.817(3)	Cd(1)–O(2)$^{\#7}$	2.400(9)
Ba(1)–O(2)$^{\#4}$	2.817(3)	Cd(1)–O(2)$^{\#10}$	2.400(9)
Ba(1)–O(1)$^{\#5}$	2.859(6)	Mean	2.309
Ba(1)–O(1)$^{\#6}$	2.859(6)		
Ba(1)–O(2)$^{\#7}$	2.913(10)	O(2)–B(1)–O(1)	121.3(5)
Mean	2.816	O(2)–B(1)–O(1)$^{\#11}$	121.3(5)
B(1)–O(2)	1.354(15)	O(1)–B(1)–O(1)$^{\#11}$	117.3(10)
B(1)–O(1)	1.397(8)	Mean	120
B(1)–O(1)$^{\#11}$	1.397(8)		
Mean	1.383		

[a] *Note*. Symmetry transformations used to generate equivalent atoms: (#1) $x+1/2, y+1/2, z$; (#2) $x+1/2, -y+3/2, z$; #3 $x, -y+2, z$; (#4) $x, y+1, z$; (#5) $-x, y, -z+1$ (#6) $-x, -y+2, -z+1$; (#7) $-x+1/2, -y+3/2, -z+2$; (#8) $-x, -y+2, -z+2$; (#9) $-x, y, -z+2$; (#10) $x-1/2, y+1/2, z$; (#11) $x, -y+1, z$.

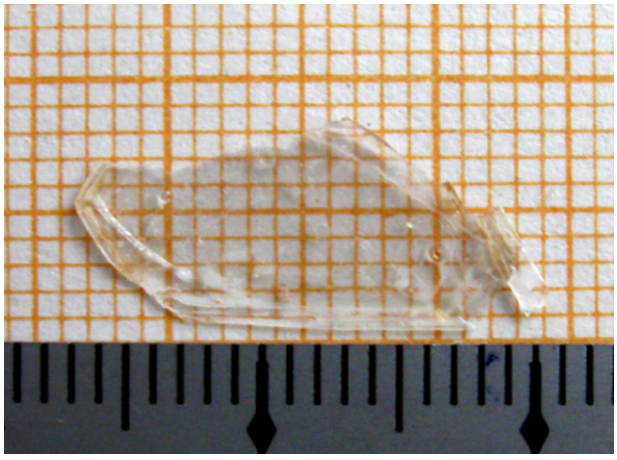

Fig. 4. The crystal photo of $Ba_2Cd(BO_3)_2$.

3.2. Comparison of the $X_2Z(BO_3)_2$ borate (X = Ba, Sr and Zn, Z = Mg, Ca, Ba and Zn)

A series of $X_2Z(BO_3)_2$ borate compounds have been reported in the literature, therein $Ba_2Ca(BO_3)_2$ [31] and $Sr_2Mg(BO_3)_2$ [32] are isostructural with $Ba_2Cd(BO_3)_2$, and all of them crystallizes in a monoclinic space group *C*2/*m*. $Ba_2Mg(BO_3)_2$ [33] has a similar crystal structure with $Ba_2Cd(BO_3)_2$, however, six Mg–O bonds in MgO_6 octahedra is 2.121 Å, forming regular octahedra in $Ba_2Mg(BO_3)_2$, whereas CaO_6 (bond lengths of 4×2.309 Å, 2×2.338 Å), MgO_6 (bond lengths of 4×2.067 Å, 2×2.144 Å) and CdO_6 (bond lengths of 4×2.262 Å, 2×2.400 Å) are distorted octahedra in $Ba_2Ca(BO_3)_2$,

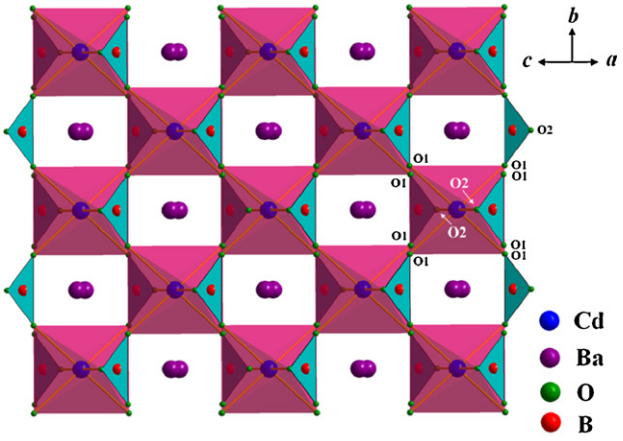

Fig. 5. Tunnel structure of $Ba_2Cd(BO_3)_2$. BO_3 triangles and CdO_6 octahedra are shaded in blue and red, respectively. (For interpretation of the references to color in this figure legend, the reader is referred to the web version of this article.)

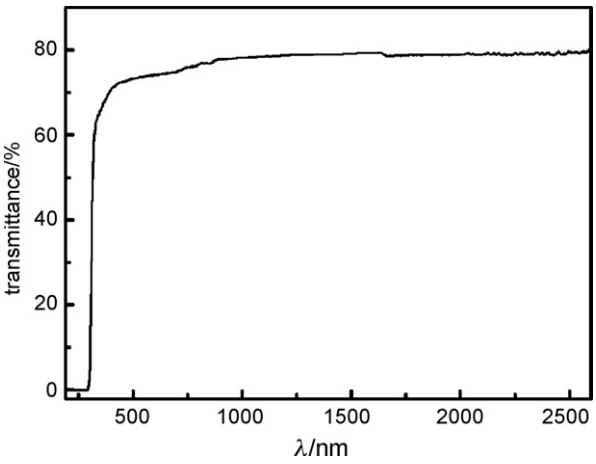

Fig. 6. Transmission spectrum of $Ba_2Cd(BO_3)_2$ crystal.

$Sr_2Mg(BO_3)_2$ and $Ba_2Cd(BO_3)_2$, respectively. Hence, $Ba_2Mg(BO_3)_2$ has a higher symmetry than three of others, and crystallizes in space group $R-3m$.

$Ba_2Zn(BO_3)_2$ [18] $BaZn_2(BO_3)_2$ [19] and $Zn_2Cd(BO_3)_2$ [20], are closely related to $Ba_2Cd(BO_3)_2$ in stoichiometry but differ in structure, crystallizes in non-centrosymmetric $R3c$, $Pca2_1$ and chiral $P2_12_12_1$ space group, respectively. The Zn analogs contain distorted ZnO_4 tetrahedra (every Zn–O bond lengths are different in the above three Zn analogs), which further connect with BO_3 to form the non-centrosymmetric crystal structure.

3.3. Crystal growth

Since the relatively high melting points of BaO and CdO in $BaO–CdO–B_2O_3$ systems, fluxes should be introduced to decrease the melting temperature and viscosity. After extensive attempts, including KF, NaF, PbO and PbF_2, etc., were tried to employ as the flux. Therein, KF and NaF were easy to cause the volatilization of reactant. Binary flux of PbO and PbF_2 can significantly reduce viscosity, so PbO and PbF_2 were adopted as fluxes. Because PbO and PbF_2 could break the B–O bonds of B_2O_3 and result the formation of $B_2O_4^{2-}$ anion, which was likely to reduce the viscosity of the system and resolve the difficulty of the thermal and physical transition. Large $Ba_2Cd(BO_3)_2$ crystals were obtained, note that the sheet-like morphology is basically owing to the intrinsic layered structure of $Ba_2Cd(BO_3)_2$.

3.4. Infrared spectrum and transmittance spectrum

In order to specify and compare the coordination of boron in $Ba_2Cd(BO_3)_2$, the infrared spectrum was measured (Fig. S1 in Supporting Information). The strong bands above 1100 cm^{-1} are mainly attributed to the BO_3 antisymmetric stretching vibrations, while those near 700 and 800 cm^{-1} should be assigned to BO_3 out of plane bending modes. Bands with the lowest frequencies below 570 mainly originate from the lattice dynamic modes [34]. The IR spectrum further confirms the existence of only trigonally coordinated boron atoms, consistent with the results obtained from the single-crystal X-ray structural analyses.

Fig. 6 shows the transmittance spectrum of the $Ba_2Cd(BO_3)_2$ crystal at room temperature. There is no absorption peak in the whole range of the spectrum, but the transmission intensity sharply decreases below 330 nm and reaches zero at about 296 nm. This means that the ultraviolet cutoff edge for the $Ba_2Cd(BO_3)_2$ crystal is 296 nm.

4. Conclusions

A novel ternary borate, $Ba_2Cd(BO_3)_2$ has been synthesized. Single crystal X-ray diffraction reveals that the basic units are BO_3, CdO_6 and BaO_9 in $Ba_2Cd(BO_3)_2$, and crystal structure is built up from the stacking of infinite stoichiometric layers along the c axis. IR spectrum and BVS calculation was used to verify the validity of the structure. The transmittance spectrum indicates that the ultraviolet cutoff edge for the $Ba_2Cd(BO_3)_2$ crystal is about 296 nm.

Acknowledgments

This work is supported by Main Direction Program of Knowledge Innovation of Chinese Academy of Sciences (Grant No. KJCX2-EW-H03-03), the "National Natural Science Foundation of China" (Grant Nos. 50802110, 21001114), the "One Hundred Talents Project Foundation Program" of Chinese Academy of Sciences, the "Western Light Joint Scholar Foundation" Program of Chinese Academy of Sciences, the "High Technology Research and Development Program" of Xinjiang Uygur Autonomous Region of China (Grant No. 200816120) and Scientific Research Program of Urumqi of China (Grant No. G09212001).

Appendix A. Supplementary data

Supplementary data associated with this article can be found, in the online version, at doi:10.1016/j.jallcom.2011.03.141.

References

[1] E.L. Belokoneva, Crystallogr. Rev. 11 (2005) 151–198.
[2] S.K. Filatov, R.S. Bubnova, Phys. Chem. Glasses 41 (2000) 216–224.
[3] C.T. Chen, Z.S. Lin, Z.Z. Wang, Appl. Phys. B 80 (2005) 1–25.
[4] S.L. Pan, J.P. Smit, B. Watkins, M.R. Marvel, C.L. Stern, K.R. Poeppelmeier, J. Am. Chem. Soc. 128 (2006) 11631–11634.
[5] P. Becker, Adv. Mater. 10 (1998) 979–992.
[6] X.Y. Fan, S.L. Pan, X.L. Hou, X.L. Tian, J. Han, Cryst. Growth Des. 10 (2010) 252–256.
[7] T. Sasaki, Y. Mori, M. Yoshimura, Y.K. Yap, T. Kamimura, Mater. Sci. Eng., R 30 (2000) 1–54.
[8] S.L. Pan, J.P. Smit, M.R. Marvel, E.S. Stampler, J.M. Haag, J. Baek, P.S. Halasyamani, K.R. Poeppelmeier, J. Solid State Chem. 181 (2008) 2087–2091.
[9] C.T. Chen, B.C. Wu, A.D. Jiang, G.M. You, Sci. Sin. Ser. B 28 (1985) 235–243.
[10] C.T. Chen, G.L. Wang, X.Y. Wang, Z.Y. Xu, Appl. Phys. B 97 (2009) 9–25.
[11] C.T. Chen, Y.B. Wang, B.C. Wu, K.C. Wu, W.L. Zeng, L.H. Yu, Nature 373 (1995) 322–324.
[12] P.S. Halasyamani, Chem. Mater. 16 (2004) 3586–3592.
[13] H.Y. Chang, S.H. Kim, K.M. Ok, P.S. Halasyamani, J. Am. Chem. Soc. 131 (2009) 6865–6873.
[14] J. Goodey, J. Broussard, P.S. Halasyamani, Chem. Mater. 14 (2002) 3174–3180.
[15] F. Li, X.L. Hou, S.L. Pan, X.A. Wang, Chem. Mater. 21 (2009) 2846–2850.
[16] W.L. Zhang, W.D. Cheng, H. Zhang, L. Geng, C.S. Lin, Z.Z. He, J. Am. Chem. Soc. 132 (2010) 1508–1509.
[17] M.R. Marvel, J. Lesage, J. Baek, P.S. Halasyamani, C.L. Stern, K.R. Poeppelmeier, J. Am. Chem. Soc. 129 (2007) 13963–13969.
[18] F. Zhang, D.Z. Shen, G.Q. Shen, X.Q. Wang, Z. Kristallogr. NCS 223 (2008) 3–4.
[19] R.W. Smith, L.J. Koliha, Mater. Res. Bull. 29 (1994) 1203–1210.
[20] R.W. Smith, D.A. Keszler, J. Solid State Chem. 100 (1992) 325–330.
[21] SAINT, Version 7.60A Bruker Analytical X-ray Instruments, Inc., Madison, WI, 2008.
[22] G.M. Sheldrick, SHELX-97: Program for Structure Refinement, University of Goettingen, Germany, 1997.
[23] L. Spek, J. Appl. Crystallogr. 36 (2003) 7–13.
[24] I.D. Brown, D. Altermatt, Acta Crystallogr. B 41 (1985) 244–247.
[25] S.F. Zhang, G.Z. Liu, S.T. Zheng, G.Y. Yang, J. Solid State Chem. 180 (2007) 1943–1948.
[26] S.L. Pan, J.P. Smit, C.H. Lanier, M.R. Marvel, L.D. Marks, K.R. Poeppelmeier, Cryst. Growth Des. 7 (2007) 1561–1564.
[27] J. Barbier, N. Penin, A. Denoyer, L.M.D. Cranswick, Solid State Sci. 7 (2005) 1055–1061.
[28] Y. Zhang, Y.D. Li, Y.S. Yin, J. Alloys Compd. 400 (2005) 222–226.
[29] J. Gou, Y.H. Wang, F. Li, J. Lumin. 127 (2007) 327–331.
[30] T.W. Kuo, T.M. Chen, J. Lumin. 130 (2010) 483–487.
[31] A. Akella, D.A. Keszler, Main Group Met. Chem. 18 (1995) 35–41.
[32] G.J. Chen, Y.C. Wu, P.Z. Fu, Acta Crystallogr. E 63 (2007) 175.
[33] A. Akella, D.A. Keszler, Mater. Res. Bull. 30 (1995) 105–111.
[34] A. Rulmont, M. Almou, Spectrochim. Acta A45 (1989) 603–610.